Overview of a 2D thrust balance used for accurate measurements of vectorized electrical thrusters

IEPC-2024-231

Presented at the 38th International Electric Propulsion Conference
Pierre Baudis Convention Center • Toulouse, France
June 23-28, 2024

P. Moutet[1], M. Zurkaulen[2], and P. Thebault[3]
Dactem International, Alès, Occitanie, 30100, France

Abstract: This paper presents a prototype of a null deflection double linear axis thrust balance designed to perform 2D measurements of the vectorization of the thrust produced by electrical thrusters. Engineering of the main features of the prototype is described, as well as experimental performances achieved by the underlying mechanical design. For this prototype, the thrust measurement ranges from few µN up to 10 mN but can easily be adapted in the future for other applications. Experimental results allowed to validate the design of the prototype, paving the way for the conception and integration of a complete 2D thrust balance.

Nomenclature

VC	=	Voice-coils
θ	=	Vectorization angle of the thrust
φ	=	Orientation angle of the thrust
G	=	Gravitational acceleration constant
O	=	Application point of the thrust
$\vec{F}$	=	Thrust vector

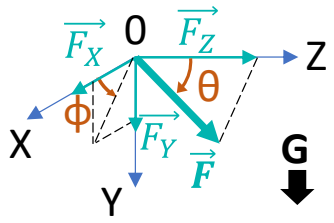

Figure 1. Thrust coordinate system

I.Introduction

ELECTRIC propulsion has been widely identified as a convenient tool for space applications for more than half a century. Its high specific impulse allows for a lighter weight than traditional chemical thrusters [1], which proves useful for a wide range of missions. In recent years, electric propulsion has seen an increase of its onboard use for small satellites, especially in the case of internet constellation ([2]). As the electrical propulsion arose, multiple thrust stands have been developed, allowing for characterization of the produced thrust. Most of these stands are designed to perform measurements of the thrust along a single axis [3], [4]. Therefore, theses stands are unable to provide analysis of the vectorization of the produced thrust. However, most of electrical thrusters display a vectorization of the produced thrust, be it intentional [5] or not [6]. In order to further improve the functionality of electrical thrusters, developing test stands able to perform measurements of the thrust along several axis is mandatory. Nowadays, only a few prototype tests stand have been integrated [7], [8], none of them allowing for a full 3D characterization of the thrust produced.

[1] Physics PhD, Electrical Engineering Department, pierre.moutet@dactem.com.
[2] Mechanical Engineer, Mechanical Engineering Department, maximilian.zurkaulen@dactem.com.
[3] Department Manager, Electrical Engineering Department, pierre.thebault@dactem.com.

In this paper, we present a prototype of a null deflection double linear axis thrust balance designed to perform 2D measurements of the vectorization of the thrust. This prototype will be paving the way for the conception and integration of a full 3D thrust stand in the future.

II. Engineering of the prototype

A. Targeted technical specification

The targeted technical specification for the 2D thrust stand has been elaborated following the feedback from several thruster manufacturers. A compromise was made on every value, in order to accommodate for most of the thrusters. An excerpt from the final specification is given in the following table.

Table 1: excerpt from the technical specification of the 2D thrust stand prototype.

Thrust measurement range	0-10 mN
Accuracy	± 50 µN
Repeatability (full scale)	≤ 50 µN
Sensitivity (full scale)	≤ 13 µN

B. Mechanical engineering

The aim of the mechanical design was to create a mechanism which allows two-dimensional movement in x- and z-axis, to provide a stiff structure and to allow for a certain minimum movement under a specified thrust.

The balance consists of four similar assemblies containing the fixed, intermediate, and free moving stage. Each axis is comprised of two opposing bearing blocks, housing the intermediate stage and all the flexure bearings. This makes for a very compact and space efficient design. Further, each block has its own mechanical end stops as well as locking system to fix the free moving part and protect the bearings. The displacement sensors and voice coil actuators are placed at the ends of each axis, fixed to the intermediate stages. Figure 2 shows an overview of the balance design.

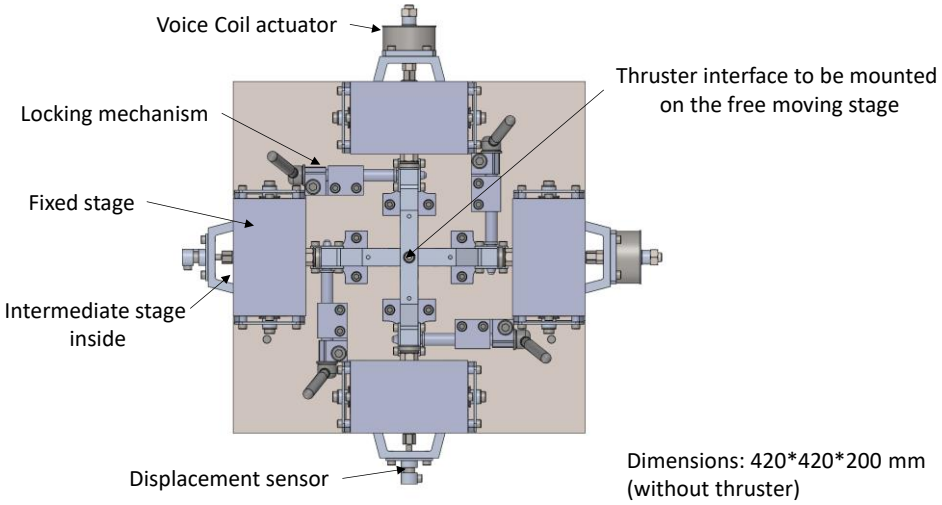

Figure 2. Overview of the 2D thrust stand

The challenge within the design were the flexure bearings which are used in this balance. The task of the bearings is to support each axis and allow frictionless movement. With these requirements, the aim is to find a good ratio between radial and axial stiffness.

For this prototype, a minimum measurable thrust of 13 µN is required. With the displacement sensor set to be a LVDT, the expected displacement under the mentioned force needed to be aligned with the measuring resolution of the sensor and its dedicated electronics. Thus, the required axial stiffness is set, being determined by the minimum thrust requirement and the according minimum deflection for accurate sensor readings. The radial stiffness is obtained by the mass of the thruster and guiding system and a minimum acceptable deformation in radial direction. The aim is to maximize the admissible thruster mass while still providing the needed displacement at given minimum thrust. In relation to the bearings' properties, this translates to maximizing the ratio between radial and axial stiffness.

To design the flexure bearings, a case study has been performed. Therefore, multiple different designs have been studied with different geometrical features. Once a suitable solution has been found, further FEM simulations as strain and stress analysis, stiffness including torsional stiffness, and others were performed to predict the behavior under load. The maximum admissible radial load is based on the allowed radial deflection as well as on the strength of the bearing material. This load was determined, and mechanical end stops were incorporated into the design to protect the bearings from overloading. This way, the system can support a thruster mass of up to 3.5 kg before going into block. After a certain deflection of the bearings, the end stops limit any further movement. Therefore, the strain and stress withing the material stay in an acceptable range to avoid damage (see Figure 3). The same concept was applied to the axial direction limiting the maximum deflection along the main axes. However, due to the big difference of axial to radial stiffness, the maximum allowed axial deflection is much higher than in radial direction.

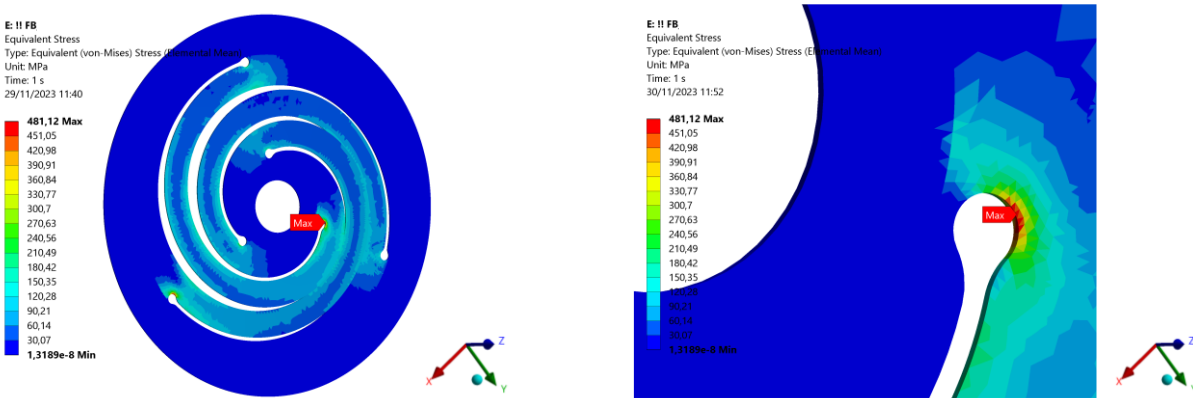

Figure 3. Stress analysis of the flexure bearing

After it was shown that the flexure bearing meets its requirements, the design was incorporated into the balance.

Following, the whole assembly was analyzed to verify the previously predicted theoretical behavior under different conditions. As anticipated, the simulation of the balance showed the expected performance yielding the calculated displacements under different forces. During the design process it was assumed that an asymmetrical load could lead to a measurement error due to induced torque. Asymmetrical load would occur if the axis of thrust is parallel but offset to either axis of the balance. This case would in theory lead to rotation of the moving part of the balance. The greater the offset, the bigger the induced torque on the balance and potential measurement error. However, it was found out that a reasonable offset-range exists in which the maximum thrust does not lead to a measurable rotation but stays within the noise. Thus, a case of problematic thrust misalignment can be ruled out when staying within the specified range.

To avoid further measuring errors, the focus was set on symmetry. Due to the nature of the design, if the flexure bearings deform asymmetrically in radial direction, the whole guiding mechanism can tilt slightly. To avoid such potential uncertainties, the guiding mechanism was balanced. Therefore, a symmetrical weight distribution was implemented. Since the voice coil assembly is heavier than the LVDT sensor, a counterweight on the sensor side was installed. This way, the center of gravity of the guiding mechanism stays in the center of the balance. This setup avoids any potential case of gravity induced thrust measurement error.

The minimum measurable thrust is set to 13 µN and the maximum to 10 mN. If the thruster has a higher thrust, the voice coil can be adapted easily. However, if a lower thrust measurement is required, more adaptation might be necessary. The displacement sensor with its electronics has to be adapted, and at a certain range as well as depending on the chosen sensors' resolution, the flexure bearings will also have to be changed.
The admissible thruster mass including interface plate is limited to 3.5 kg. Any higher mass will lead to a blockage of the guiding system due to overload protection, on the other hand, smaller masses can always be supported. If, however, the thruster mass needs to be increased, the flexure bearings will also have to be adapted for higher radial loads. The design offers the possibility to use different types of flexure bearings thus offering a wide range of potential use cases.

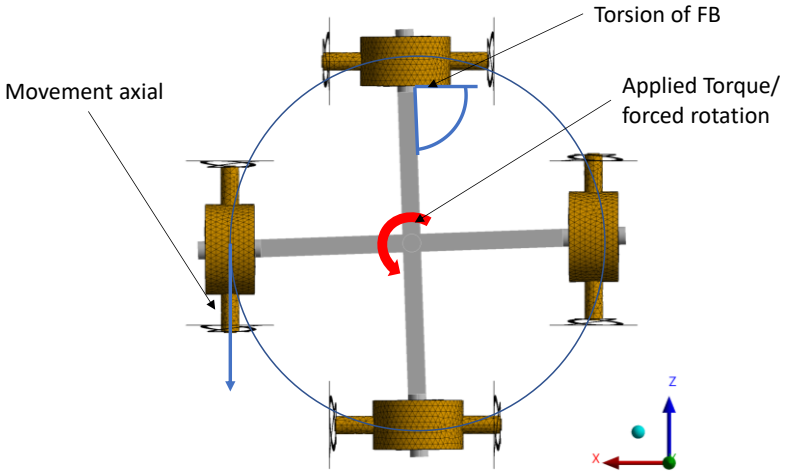

Figure 4. Exaggerated rotational behavior of the balance under forced rotation

To improve handling and operations, a system to block the balance is integrated. This consists of four sliding pins which can block each side of the moving stage independently. When handling the balance, including transporting or mounting of the thruster on top, the lock can be used to avoid unintentional movement of the guiding system. Further it supports the flexure bearings by removing any load of handling operations. For a future model it is anticipated to include an electric variant to improve handling even more.

C. Actuators engineering

The VC integrated inside the thrust stand has been heavily inspired by an existing one previously designed and integrated in a thrust balance [4]. The coil of the VC has been adapted in order to allow for a reduction of the produced force.

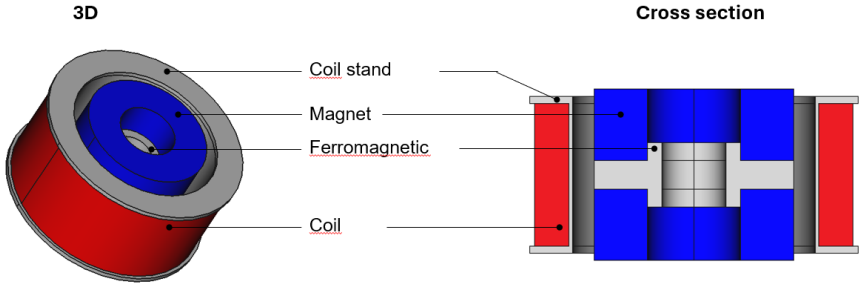

Figure 5. Design of the integrated VC

The current design of the VC features an external diameter of 4.7 cm, with a length of 2.4 cm. The coil is fitted with 108 windings of AWG 20 copper wire. Using a current ranging from few µA to 100 mA allows the production of a force from few µN to 10 mN. This result has been achieved using Sm2Co-17 magnets, allowing for a very strong magnetic field of 2T within the ferromagnetic parts of the VC.
This design ensures the possibility to produce 10 mN force without any significant Joule heating (44 mW).

III. Experimental results

A picture of the mechanics of the 2D thrust stand after integration is presented in Figure 6. As planned, the thrust stand dimensions are comprised within a box of 420 by 420 by 200 cm (without the electrical thruster). During testing, the thrust stand is mounted on an optic marble table, for stability. The inclination of the prototype is adjusted using a tripod in order to achieve good horizontality (±1°) of the central plate where the thruster is to be fitted. Mechanical interface are available on the central plate of the thrust stand in order to accommodate any kind of electrical thruster.

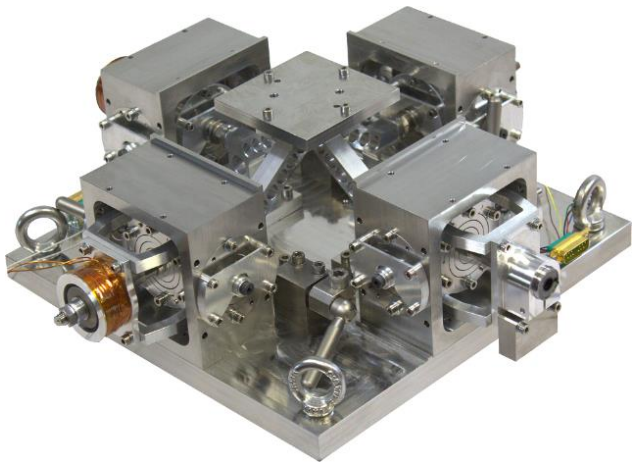

Figure 6. Picture of the 2D thrust stand prototype.

A. Mechanical results

1. Stiffness

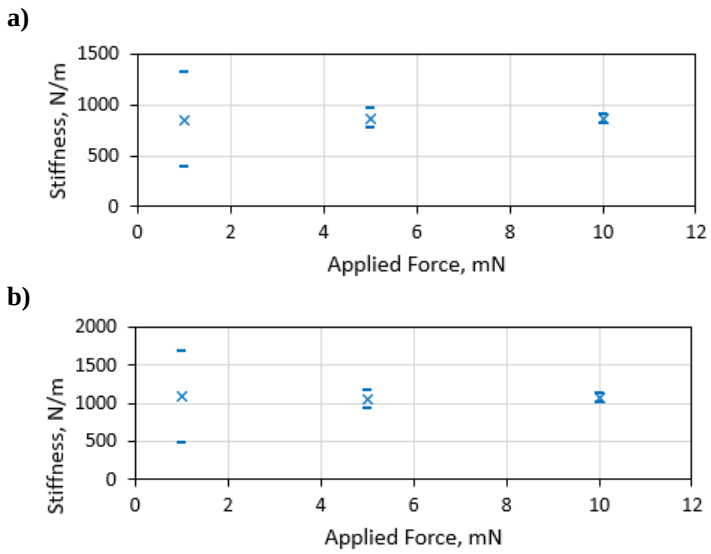

Figure 7. Variation of the axial stiffness along the a) X and b) Z axis.

For this experiment, a controlled force has been applied using and external calibration tool, ranging from 1mN up to 10 mN. The displacement of the axis is then measured, using a displacement sensor integrated within the thrust stand.

Experimental results of the variation of the axial stiffness along the X and Z axis are presented respectively in Figure 7 a) and b). Measurements are represented by a cross, while the error margins are represented by dashes. The error margin for 1 mN Applied Force is ±597 N/m, while it is only of ±58 N/m for an Applied Force of 10 mN. This is caused by a constant margin error on the Applied Force of ±550 µN, due to limitations of the external calibration tool used to calibrate the VCs. Nevertheless, it appears clearly from these measurements that the stiffness along both axes stays constant respectively to the Applied Force. This indicates that the mechanical displacement is operating as designed, without any sort of dry friction appearing during movement.

2. Dynamical behaviour

For this experiment, using the integrated VC, an initial displacement is applied to one of the axes. The current is then stopped and the resulting oscillations of the position of the axis is acquired. Figure 8 displays the result obtained for the X axis. At the start of the experiment, an initial displacement of +12 µm has been applied. After stopping the current, the position of the moving part is quickly oscillating at 3.4 Hz, with 90% attenuation of the oscillations obtained after 10 s. This stabilization time is without any added dampening which could be achieved by various means, such as activating a regulation of the position (PID), or by adding a specific hardware equipment (magnets, coils, and so on).

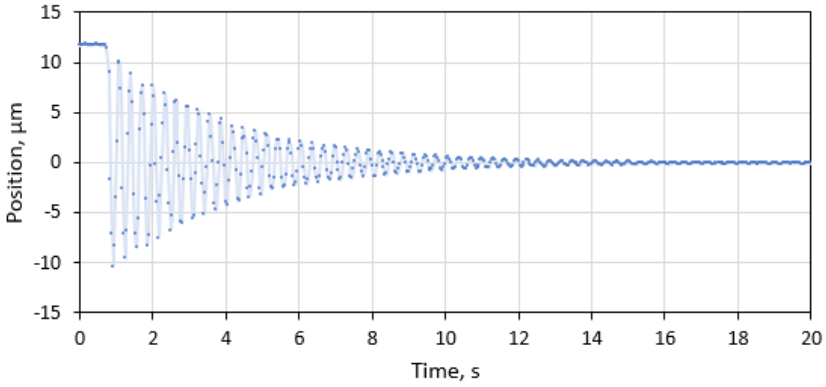

Figure 8. Free oscillations of the position along the X axis.

Similar results have been obtained for the Z axis. As such, these results indicated once again that the mechanical displacement is behaving as intended, without dry friction. The stabilization time is also compatible with a reasonable (<10 s.) acquisition time and could be even further improved by adding some dampening.

3. Impact of the applied weight to the mechanical results

This experiment is similar to the one presented in Figure 8, although weights were added on top of the central plate, in order to simulate electrical thrusters of various masses. Figure 9 presents the results obtained.

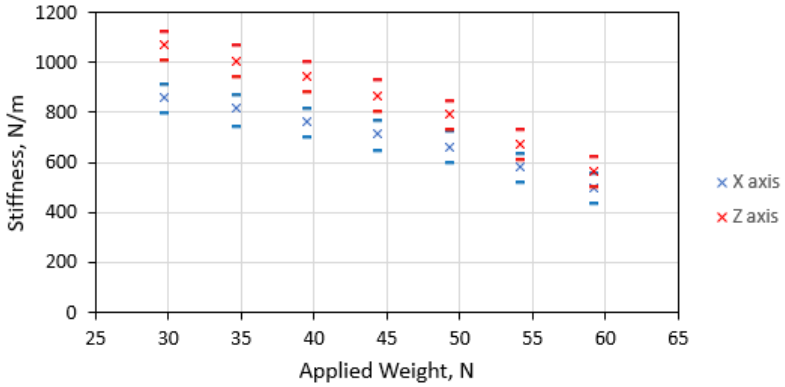

Figure 9. Variation of stiffness of X and Z axis with the Applied Weight (payload)

The red and blue crosses represent the experimental data respectively for the Z and X axis, and the dashes represent the error margin. It can be noted that the stiffness of both X and Z axis at 29 N are very close – respectively 860 N/m and 1069 N/m. The existence of a slight difference can be explained by some variations of some of the mechanical parts. The stiffness is decreasing down to 504 N/m (X axis) and 564 N/m (Y axis) for an applied total weight of 59 N – which would be equivalent to an electrical thruster of about 3.5 kg (the rest of the 2.5 kg being the weight of the moving parts of the thrust stand itself). This decrease is highly in our favor regarding the future performances of the thrust stand. Indeed, with a reduced stiffness, the displacement for a given thrust will be higher, thus easier to detect with a displacement sensor. This would help improve the performances of the repeatability, sensitivity and resolution of the thrust stand.

B. Thrust measurement results

For this experiment, an externally controlled force (Applied Thrust) was applied to the thrust stand, and the resulting measurement from the thrust stand was acquired (Measured Thrust). Comparison between the two allowed to analyze the performances of the thrust stand. Figure 10 present the results for both measurement axis.

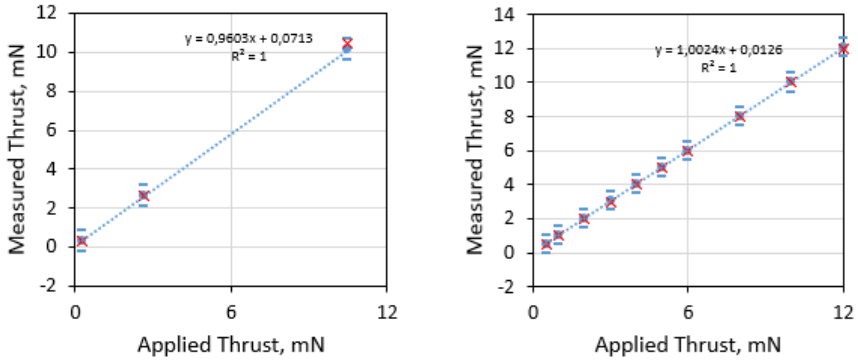

Figure 10. Performances of thrust measurement for X axis (left) and Z axis (right)

As it has been previously stated, the error margin of the Applied Thrust is ±550 µN, therefore the calibration of the thrust stand is also integrating this error margin. Despite this significant error margin, both axes display good correlation between the Applied Thrust and the Measured Thrust. The red crosses represent perfect correlation (idealization), and it can be observed that the actual measurements (blue dots) are very closely located to the red cross. This indicates that both axes are well performing. As expected, results are fitted by a linear regression, which indicates that performances of the thrust measurements are similar throughout the whole range (0-10 mN).

IV. Conclusion

A 2D thrust stand prototype based on two interconnected linear axes has been designed and integrated. The targeted performances and the chosen mechanical design of the final 2D thrust stand has been presented.

After integration of a prototype, behavior and performances of the mechanisms has been studied, which includes stiffness of each axis, impact of the thruster weight, response time, and thrust measurements performances. Obtained results are excellent and will pave the way for the realization of a finalized version of the 2D thrust stand prototype which will be able to validate the targeted performances previously established. In turn, this 2D thrust stand will itself be a significant progression toward a full 3D thrust balance.

V. Acknowledgement

The work presented in this paper has been achieved with the trust, support and funding of CNES as part of their R&T.

[1] P. Erichsen, « Performance Evaluation of Spacecraft Propulsion Systems in Relation to Mission Impulse Requirements », vol. 398, p. 189, août 1997.
[2] « Starlink | Technologie », Starlink. Consulté le: 18 juin 2024. [En ligne]. Disponible sur: https://www.starlink.com/technology
[3] U. Kokal, « Development of a Mili-Newton Level Thrust Stand for Thrust Measurements of Electric Propulsion Systems and UK90 Hall Effect Thruster », 2018.
[4] P. Moutet et E. Pouleau, « OVERVIEW OF AN OPTIMIZED THRUST BALANCE USED FOR ACCURATE MEASUREMENTS IN ELECTRICAL THRUSTER QUALIFICATION ENDURANCE TESTING ».
[5] N. Leveque, « TRAJECTORY SIMULATIONS FOR THRUST-VECTORED ELECTRIC PROPULSION MISSIONS ».
[6] M. Kakano'and et Y. Arakasvat, « Trajectory Analysis of Electric Propulsion System with Thrust Misalipment ».
[7] E. Gourcerol, V. Désangles, D. Packan, et F. Gaboriau, « Design of a 2-axis thrust stand for thrust vectoring diagnostics of an ECR thruster », in *EUCASS-CEAS 2023*, Lausanne, Switzerland, juill. 2023. doi: 10.13009/EUCASS2023-731.
[8] N. Nagao, S. Yokota, K. Komurasaki, et Y. Arakawa, « Development of a two-dimensional dual pendulum thrust stand for Hall thrusters », *Rev. Sci. Instrum.*, vol. 78, nº 11, p. 115108, nov. 2007, doi: 10.1063/1.2815336.